ARTICLE

JAAS
www.rsc.org/jaas

High-precision Cu and Zn isotope analysis by plasma source mass spectrometry
Part 1. Spectral interferences and their correction

Thomas F. D. Mason,*[a] Dominik J. Weiss,[a,b] Matthew Horstwood,[c] Randall R. Parrish,[c,d] Sara S. Russell,[b] Eta Mullane[b] and Barry J. Coles[a]

[a]*Department of Earth Science and Engineering, Imperial College London, UK SW7 2BP. E-mail: thomas.mason@ic.ac.uk; Fax: 0207 594 7444; Tel: 0207 59 46395*
[b]*Department of Mineralogy, Natural History Museum, London, UK SW7 5BD*
[c]*NERC Isotope Geosciences Laboratory, Keyworth, Nottinghamshire, UK NG12 5GG*
[d]*Department of Geology, University of Leicester, University Road, Leicester, UK LE1 7RH*

Received 18th June 2003, Accepted 18th November 2003
First published as an Advance Article on the web 20th January 2004

Spectral interferences originating from instrumental and sample-matrix components continue to present a major analytical challenge to high-precision isotope ratio measurements by multiple-collector inductively coupled plasma mass spectrometry (MC-ICP-MS). This is particularly true when measuring stable isotopic variability of Cu and Zn, where instrumental and sample-matrix related spectral components may obscure the very small isotopic anomalies that typify these metals in terrestrial materials. We present a systematic characterisation and quantification of spectral interferences across the mass range ^{63}Cu to ^{70}Zn using two MC-ICP-MS instruments: a Micromass IsoProbe and a VG Axiom. Significant instrumental Ni backgrounds of up to 40 mV total Ni occur on the IsoProbe, reflecting streaming off the Ni-sampler and/or skimmer cones. This Ni contribution, however, is insufficient to account for the excess peak contribution at ^{64}amu, suggestive of an as yet unidentified interference contribution at this mass. By contrast, Ni backgrounds on the Axiom are roughly one order of magnitude lower, and no comparable interference occurs at ^{64}amu. High-resolution mass scans on the Axiom have identified $^{40}Ar^{12}C^{16}O^+$ and $^{40}Ar^{14}N^{14}N^+$ species at ^{68}amu and $^{40}Ar^{14}N^{16}O^+$ at ^{70}amu. Also, HNO_3-related $^1H^1H^{14}N^{16}O^{16}O^{16}O^+$ and $^1H^1H^{14}N^{16}O^{16}O^{18}O^+$ species at ^{64}amu and ^{66}amu respectively were observed on the Axiom using solution nebulisation. None of these species were observed on the IsoProbe, possibly reflecting the effect of an Ar-bled hexapole collision cell that reduces molecular interferences through ion-molecule reactions. Instrumental backgrounds have been successfully corrected using an on-peak acid blank subtraction procedure. Zinc hydride adducts occur on the Axiom using solution nebulisation. These interferences are eliminated using a desolvated plasma, and have been corrected by monitoring the $^{64}Zn^1H^+/^{64}Zn$ ratio on a pure Zn solution and applying an offline peak subtraction. No Zn hydride interferences were observed on the IsoProbe, suggesting differences in instrument design influence the formation and/or persistence of these species. Matrix-induced interference contributions on the Axiom and IsoProbe show increasing significance from argides ($NaAr^+$, $MgAr^+$, $AlAr^+$) to oxide/hydroxide (TiO^+, $TiOH^+$, VO^+, VOH^+, CrO^+, $CrOH^+$) to double-charged species (Ba^{2+}, Ce^{2+}). Switching from solution nebulisation to a desolvated plasma enhances argide and double-charge species, and concurrently depresses oxides and hydroxides, reflecting changing conditions within the ICP-source. These results highlight the importance of removing problematic matrix components prior to Cu and Zn MC-ICP-MS isotope ratio measurements.

Introduction

By combining the enhanced ionisation efficiency of an inductively coupled plasma (ICP) source with the high precisions attainable from a multiple-collector (MC) Faraday array, MC-ICP-MS has revolutionised the study of radiogenic and stable isotope systems alike.[1–4] A prime example of this is the recent growth in the field of Cu and Zn stable isotope geochemistry, where MC-ICP-MS has enabled routine analysis of terrestrial mass-dependent isotopic anomalies for the first time.[5–9] MC-ICP-MS remains, however, a relatively new technique, and the complexities related to using these instruments for high-precision isotope ratio measurements are only now becoming apparent.[3,10,11] A thorough assessment of the uncertainties associated with MC-ICP-MS Cu and Zn isotope ratio measurements is therefore warranted to both assure data quality and ultimately improve upon the current levels of precision and accuracy attainable.

Two obstacles must be overcome when measuring Cu and Zn isotope ratios by MC-ICP-MS: (1) spectral interferences, the focus of this paper, and (2) non-spectral mass discrimination effects, as addressed in a companion paper.[12] Spectral interferences from elemental isobars, major argides, trace oxides and doubly-charged species are common throughout the Cu–Zn mass range (see Table 1). With Magnetic Sector ICP-MS instruments, spectral interferences can be resolved from their associated Cu and Zn peaks by increasing mass resolution to *ca.* $M/\Delta M = 3000$, as has been successfully used for ultra-trace analysis of Cu and Zn directly within biological and environmental samples.[13–18] However, increasing mass resolution concurrently decreases signal transmission and leads to rounding of peak shapes, both of which compromise high-precision isotope ratio measurements. Furthermore, not all MC-ICP-MS instruments are capable of high-resolution isotope ratio measurements, and increasing mass resolution is not always applicable.

DOI: 10.1039/b306958c

Table 1 List of potential interfering species[a] across the mass range ^{60}amu to ^{70}amu

Mass	Monoisotopic species	Argides	Oxides	Double-charged species[b]	Elemental species
60.0	^{60}Ni (26.1)	$Ar^{20}Ne$ (90.3)	^{44}CaO (2.09)	$^{120}Sn^{2+}$ (32.3), $^{120}Te^{2+}$ (0.10)	
60.5				$^{121}Sb^{2+}$ (57.3)	
61.0	^{61}Ni (1.13)	$Ar^{21}Ne$ (0.27)	^{45}ScO (99.8)	$^{122}Sn^{2+}$ (4.63), $^{122}Te^{2+}$ (2.60)	
61.5				$^{123}Sn^{2+}$ (42.7), $^{123}Te^{2+}$ (0.91)	
62.0	^{62}Ni (3.59)	$Ar^{22}Ne$ (9.18)	$^{23}Na^{23}NaO$ (99.8), ^{46}TiO (7.98)	$^{124}Sn^{2+}$ (5.79), $^{124}Te^{2+}$ (4.82), $^{124}Xe^{2+}$ (0.10)	$^{31}P^{31}P$(100)
62.5				$^{125}Te^{2+}$ (7.14)	
63.0	^{63}Cu (69.2)	$Ar^{23}Ne$ (99.6)	$^{31}PO_2$ (99.5), ^{47}TiO (7.28), $^{47}TiOH$ (7.98)	$^{126}Te^{2+}$ (19.0), $^{126}Xe^{2+}$ (0.09)	
63.5				$^{127}I^{2+}$ (100)	
64.0	^{64}Zn (48.6), ^{64}Ni (0.91)	$Ar^{24}Mg$ (78.7), $Ar^{12}C^{12}C$ (97.4)	$^{32}SO_2$ (94.6), ^{48}CaO (0.19), ^{48}TiO (73.6), $^{47}TiOH$ (7.98)	$^{128}Te^{2+}$ (31.69), $^{128}Xe^{2+}$ (1.91)	$^{32}S^{32}S$ (90.3)
64.5				$^{129}Xe^{2+}$ (26.4)	
65.0	^{65}Cu (30.8)	$Ar^{25}Mg$ (9.96), $Ar^{12}C^{13}C$ (2.17)	$^{32}SO_2H$ (94.6), ^{49}TiO (5.49), $^{48}TiOH$ (73.6)	$^{130}Te^{2+}$ (33.8), $^{130}Xe^{2+}$ (4.10), $^{130}Ba^{2+}$ (0.11)	$^{33}S^{33}S$ (1.43)
65.5				$^{131}Xe^{2+}$ (21.2)	
66.0	^{66}Zn (27.6)	$Ar^{26}Mg$ (11.0)	$^{34}SO_2$ (4.19), $^{49}TiOH$ (5.49), ^{50}TiO (5.39), ^{50}CrO (4.34), ^{50}VO (0.24)	$^{132}Xe^{2+}$ (26.9), $^{132}Ba^{2+}$ (0.10)	$^{32}S^{34}S$ (8.00)
66.5				$^{133}Cs^{2+}$ (100)	
67.0	^{67}Zn (4.10)	$Ar^{27}Al$ (99.6)	$^{35}ClO_2$ (75.4), $^{34}SO_2H$ (4.19), $^{50}TiOH$ (5.49), $^{50}CrOH$ (4.34), ^{51}VO (99.5), ^{50}VOH (0.24)	$^{134}Xe^{2+}$ (10.4), $^{134}Ba^{2+}$ (2.42)	
67.5				$^{135}Ba^{2+}$ (6.56)	
68.0	^{68}Zn (18.8)	$Ar^{28}Si$ (91.6), $Ar^{12}CO$ (98.3), $Ar^{14}N^{14}N$ (98.9)	$^{35}ClO_2H$ (75.4), ^{52}CrO (83.6), ^{51}VOH (99.5)	$^{136}Xe^{2+}$ (8.90), $^{136}Ba^{2+}$ (7.85), $^{136}Ce^{2+}$ (0.19)	
68.5				$^{137}Ba^{2+}$ (11.2)	
69.0	^{69}Ga (60.1)	$Ar^{29}Si$ (4.65)	$^{37}ClO_2$ (24.1), ^{53}CrO (9.48), $^{52}CrOH$ (83.6)	$^{138}Ba^{2+}$ (71.7), $^{138}Ce^{2+}$ (0.25), $^{138}La^{2+}$ (0.09)	
69.5				$^{139}La^{2+}$ (99.9)	
70.0	^{70}Zn (0.60), ^{70}Ge (20.50)	$Ar^{30}Si$ (3.09), $Ar^{14}NO$ (99.0)	$^{37}ClO_2H$ (24.1), ^{54}CrO (2.36), $^{53}CrOH$ (9.48), ^{54}FeO (5.79)	$^{140}Ce^{2+}$ (11.1)	$^{35}Cl^{35}Cl$ (57.4)

[a] The relative proportion of each isobaric interference as a percentage of the total interference contribution for that species is given in parentheses as calculated using Element2 Interference Workshop Version 2.5 software (Finnigan MAT GmbH, Bremen, Germany). Interferences incorporating minor isotopes of O and Ar have been excluded for simplicity. Unless otherwise specified, the charge of the interference is +1. [b] Significant Sn, Sb, Te, Xe, I and Cs double-charged species are not expected due to the high second ionisation potentials of these elements.

Because of the very high-precisions required to measure natural mass-dependent isotopic anomalies of Cu and Zn of typically below ± 100 ppm (2σ),[5–9] it is imperative that interference contributions originating from both instrumental and sample-related sources during MC-ICP-MS measurements are quantified at low resolution (*ca.* $M/\Delta M = 400$–500). Consequently, a systematic evaluation of spectral interference contributions across the Cu–Zn mass range has been undertaken on two MC-ICP-MS instruments: a VG Axiom and a Micromass IsoProbe. Fundamental differences exist in the design of these instruments; the Axiom employs an electrostatic analyser to focus ion energies, while the IsoProbe uses a hexapole collision cell, with argon as the collision gas, to reduce the spread of ion energies. Comparing the Axiom and IsoProbe thus provides insights into how contrasting interface designs and ion-focussing technologies influence the generation and persistence of interfering ions across the Cu–Zn mass range. In addition, two sample introduction methodologies (a micro-concentric nebuliser and spray chamber set-up, and a desolvating nebuliser system) have been assessed on both MC-ICP-MS instruments, providing insights into how changing plasma conditions control the formation of polyatomic species.

Within this framework, instrumental and sample-related spectral interference contributions have been described and quantitatively assessed, and procedures for their correction developed. Together these results provide a foundation from which protocols for high-precision Cu and Zn measurements in natural materials are currently being developed, as will be the focus of subsequent publications.

Experimental

Experimental details of the reagents and standards, instrumental set-up, and measurement protocols used during both this study and a companion study[12] are given below. It should be noted that not all of the information given in the section is directly relevant to this study.

Reagents and standards

Four Zn and three Cu high-purity standards were used during the study: (1) an in-house 1000 μg ml^{-1} Zn standard prepared from a Johnson Matthey Purotronic Zn metal (supplied through Alfa Aesar, Karlsruhe, Germany) batch no. NH 27040 (Ref. IMP Zn), (2) a 10 000 μg ml^{-1} Zn standard supplied by Maréchal *et al.*[6] (Ref. JMC Zn), (3) a 1000 μg ml^{-1} PrimAg™ ROMIL ICP-MS Zn standard (ROMIL Ltd., Cambridge, UK) (Ref. Romil Zn), (4) a 1000 μg ml^{-1} Specpure ICP-MS Zn standard (Alfa Aesar, Karlsruhe, Germany) (Ref. Spec pure Zn), (5) an in-house 1000 μg ml^{-1} Cu standard prepared from a Johnson Matthey Purotronic Cu foil (supplied through Alfa Aesar, Karlsruhe, Germany) batch No. W15081 (Ref. IMP Cu), (6) a 1000 μg ml^{-1} Cu solution prepared from the certified reference material NIST-SRM 976 (Ref. NIST Cu) and (7) a 1000 μg ml^{-1} Cu standard supplied by Maréchal *et al.*[6] (Ref. JMC Cu). JMC Zn and JMC Cu were originally prepared from Johnson Matthey metal and represent batch No. 3-0749 L and 400882 B, respectively. Single element ICP-MS standards for P, S, Na, Mg, Mn, Ca, Ti, V, Cr, Sn, Te, Ba and Ce (BDH Laboratory Supplies, Poole, UK) were also used. All working solutions were prepared in ultra-pure sub-boiling acids (ROMIL Ltd., Cambridge, UK) using >18.2 MΩ cm H_2O from a Milli-Q water system (Millipore Corporation, Bedford, MA, USA). Solutions were prepared under laminar flow cabinets following clean laboratory procedures.

Instrumentation

Two MC-ICP-MS systems were used for the study: a VG Axiom (Thermo Elemental, Cheshire, UK) based at the NERC Isotope Geosciences Laboratory, Keyworth, UK, and a Micromass IsoProbe (GV Instruments, Manchester, UK) which forms part of the joint analytical facility between Imperial College and the Natural History Museum, London, UK. Detailed instrumental-type descriptions are given elsewhere.[3]

Three sample introduction systems were used: (1) a micro-uptake T1-H type nebuliser with an Aridus membrane desolvation system (CETAC Inc., Omaha, NE, USA) with both the Axiom and IsoProbe, (2) a micro-concentric low-uptake nebuliser with a cyclonic-impact-bead spray chamber combination with the Axiom, and (3) a micro-concentric low-uptake nebuliser with a Scott double-pass spray chamber with the IsoProbe. Free air aspiration was used throughout. For the purpose of the discussion, (1) is referred to as dry plasma, while (2) and (3) are referred to as wet plasma. However, whilst the Aridus desolvates solutions by $>95\%$,[19] a small proportion of water continues to enter the plasma and in the strictest sense this is not a truly dry plasma.

Measurement protocols and experimental design

Typical instrumental running conditions and elemental sensitivities are given in Table 2. Measurements on the IsoProbe were made in hard extraction mode where the extraction voltage applied to the rear of the skimmer was maintained at *ca.* -400 V. Unless otherwise specified, isotope ratio measurements were made in static multi-collection mode using the collector configurations listed in Table 2. ^{70}Zinc was not measured on either instrument owing to limitations imposed by the collector configurations used. Runs comprised 25–200 five-second-integrations. Baselines were corrected using one of two procedures depending upon requirements: (1) 10 s off-peak baseline measurements (amu $\pm$ 0.5 on the Axiom and amu $\pm$ 0.25 on the IsoProbe) taken prior to each analysis, and (2) acid blank analyses of one block of 25 measurements taken before each analysis and used for an on-peak-zero baseline subtraction. All data processing was done off-line.

High-resolution scans ($M/\Delta M = 3500$ to 10 000) were used on the Axiom to resolve polyatomic interferences from residual Cu and Zn backgrounds. Sample matrix-related polyatomics were identified through analysing a series of elemental solutions (0.1 μg ml^{-1} of S, P, Ca, Na, Mg, Al, Si, Mn, Ti, V, Cr, Sn, Te, Ba or Ce spiked with 0.01 μg ml^{-1} Cu and Zn in 2% (v/v) HNO_3). These elements were chosen because they are important constituents of polyatomic interferences in the Cu–Zn mass range (see Table 1). Relative interference contributions were subsequently calculated by ratioing the maximum peak intensity of the identified interference and its associated Cu or Zn peak, providing a semi-quantitative estimate of the relative interference contribution.

Because of the fixed mass resolution ($M/\Delta M = 500$) of the IsoProbe used in this study, high-resolution scans were not possible. Consequently, sample matrix-related interferences were assessed by comparing a series of matrix-matched 0.1 μg ml^{-1} Cu and 0.1 μg ml^{-1} Zn solutions spiked with 1 μg ml^{-1} of S, P, Ca, Na, Mg, Al, Si, Mn, Ti, V, Cr, Sn, Te, B or Ce to the unspiked Cu and Zn solution following a sample-standard bracketing protocol. Relative shifts between the on-peak baseline corrected Cu and Zn isotopic compositions of the spiked and standard solutions were subsequently interpreted to represent spectral interferences incorporating the associated matrix element following Shao and Horlick.[20] This does not account for matrix-related mass discrimination effects, and thus is considered a semi-quantitative estimate.

Table 2 Operating conditions and collector configurations used on the Axiom and IsoProbe

	VG Axiom	Micromass IsoProbe
Instrumental parameters		
Coolant Ar flow	15 l min^{-1}	14 l min^{-1}
Auxiliary Ar flow	1.2−1.7 l min^{-1}	1.0−1.4 l min^{-1}
Nebuliser Ar flow	0.75−0.95 l min^{-1}	0.69−0.80 l min^{-1}
Collision cell Ar flow	–	1.2–1.4 μl min^{-1}
Ion energy	4950 V	6000 V
Torch power	1250 W forward (<10 W reflection)	1336 W forward (<10 W reflection)
Cones	Pt tipped Ni Sample + Ni Skimmer	Ni Sample + Ni Skimmer
Nebuliser parameters		
Aridus		
Spray chamber temp	+70 °C	+70 °C
Desolvator temp.	+160 °C	+160 °C
Ar sweep gas flow	3.5–5.0 l min^{-1}	2.5–3.5 l min^{-1}
Sample uptake rate	*ca.* 50 μl min^{-1}	*ca.* 50 μl min^{-1}
Sensitivity[a]	*ca.* 35 V/μg ml^{-1} Cu and Zn	*ca.* 10 V/μg ml^{-1} Cu and Zn
Micro-concentric		
Spray chamber type	Cyclonic + impact-bead set-up	Scott double-pass
Spray Chamber temp.	10 °C	4 °C
Sample uptake rate	*ca.* 400 μl min^{-1}	*ca.* 400 μl min^{-1}
Sensitivity[a]	*ca.* 40 V/μg ml^{-1} Cu; *ca.* 18 V/μg ml^{-1} Zn	*ca.* 8 V/μg ml^{-1} Cu; *ca.* 5 V/μg ml^{-1} Zn

Collector configuration

Position	L4	L3	L2	L1	Ax	H1	H2	H3	H4	H5	L4	L3	L2	L1	Ax	H1	H2	H3	H4	H5
Mass (Faraday)	62	–	63	64	65	66	67	67.5	68	–	–	–	63	64	64.5	65	66	67	67.5	68
Mass (Ion-counter)[b]	–	–	–	–	–	–	–	–	–	–	–	60	–	–	–	–	–	–	–	–
Mass resolution	Variable from $M/\Delta M$ = 400 to 10 000 (set to 400 for ratio measurements)										Fixed at $M/\Delta M$ = 500									

[a] Sensitivity values give the total ion beam signals in volts for the analysis of a 1 μg ml^{-1} Cu + 1 μg ml^{-1} Zn elemental solution. [b] With the exception of ^{60}amu that was monitored using a Channeltron ion-counter (IC), all isotope ratios were measured using Faraday detectors. The IC was cross-calibrated to the Faraday array using a peak jumping protocol, whereby the instrumental ^{60}Ni contribution measured on a 0.2% (v/v) HNO_3 acid blank was sequentially switched between the IC and L2 Faraday.

Results and discussion

Background interferences—elemental isobars

Two elemental isobars occur in the Cu–Zn mass range: ^{64}Ni on ^{64}Zn and ^{70}Ge on ^{70}Zn. While no significant Ge contributions were observed on either the Axiom or IsoProbe during this study, Ni backgrounds occur, with total Ni contributions under wet plasma conditions exceeding 2.5 mV and 15 mV, respectively. These Ni contributions are independent of the sample introduction matrices analysed (2% (v/v) HNO_3, 0.2% (v/v) HNO_3 and Milli-Q H_2O) and persist when no solution is introduced to the plasma. This indicates the Ni originates within the instruments, with the Ni skimmer and sampler cones being the probable source. Nickel backgrounds increase using dry plasma conditions, to 5 mV on the Axiom, and 40 mV on the IsoProbe. This behaviour is consistent with the higher temperature of the dry plasma, which enhances the release of Ni from the interface region. The lower Ni backgrounds on the Axiom may reflect the use of a Pt-tipped sampler cone. However, provisional measurements substituting this with a Ni-sampler observed no significant increase in Ni backgrounds, suggesting the sampler cone is not the dominant source of Ni within the Axiom.

Ni contributions measured at ^{62}amu and ^{60}amu have been used to correct off-peak baseline corrected 0.2% HNO_3 acid blank data for instrumental ^{64}Ni on the Axiom and IsoProbe, respectively. This correction assumes the instrumental Ni contribution has an isotopic composition that approximates to natural abundance values[21] and that the mass discrimination behaviour of Ni approximates to the exponential law.[22] For the Axiom, Ni-corrected ^{66}Zn/^{64}Zn acid blank data approximate to the natural abundance composition of Zn[21] for both wet and dry plasma measurements, suggesting no additional interfering species other than Ni occur on either ^{64}amu or ^{66}amu. By contrast, Ni-corrected ^{66}Zn/^{64}Zn acid blank data collected on the IsoProbe give values that are significantly below Zn natural abundance values for both wet and dry plasma conditions, and a similar shift of the same magnitude occurs for Ni-corrected ^{68}Zn/^{64}Zn acid blank data. Together these results provide evidence for an additional spectral interference on ^{64}amu.

Several polyatomic species coincide with ^{64}amu including $^{40}Ar^{24}Mg^+$, $^{36}Ar^{28}Si^+$, $^{48}Ca^{16}O^+$, $^{48}Ti^{16}O^+$, $^{32}S^{16}O^{16}O^+$, $^{32}S^{32}S^+$, $^{128}Xe^{2+}$ and $^{40}Ar^{12}C^{12}C^+$. Of these, $^{40}Ar^{24}Mg^+$, $^{36}Ar^{28}Si^+$, $^{48}Ca^{16}O^+$, $^{48}Ti^{16}O^+$, $^{32}S^{16}O^{16}O^+$, $^{32}S^{32}S^+$ and $^{128}Xe^{2+}$ have been discounted owing to the lack of associated interferences that incorporate constituent isotopes of differing mass (*e.g.* $^{40}Ar^{25}Mg^+$ at ^{65}amu). Furthermore, consistency between ^{68}Zn/^{64}Zn and ^{66}Zn/^{64}Zn ratio data indicates no additional $^{40}Ar^{12}C^{16}O^+$ interference is present at ^{68}amu on the IsoProbe, suggesting Ar + C polyatomics do not form in significant quantities. An additional species that potentially occurs is $^{16}O_4{}^+$, originating from water molecules within the hexapole collision cell. However, there remains no direct evidence to support the presence of $^{16}O_4{}^+$, and additional work is required to test this hypothesis.

Background interferences—plasma-related polyatomics

High-resolution mass scans on the Axiom have identified $^{40}Ar^{14}N^{14}N^+$, $^{40}Ar^{12}C^{16}O^+$ and $^{40}Ar^{14}N^{16}O^+$ interferences at ^{68}amu and ^{70}amu (see Fig. 1). Changing from wet to dry plasma conditions incurred a ten-fold decrease in $^{40}Ar^{14}N^{16}O^+$ (see Fig. 1(b)), as is consistent with a reduction in the amount of oxygen entering the plasma in response to the desolvation process. In contrast, no significant reductions in $^{40}Ar^{14}N^{14}N^+$ or $^{40}Ar^{12}C^{16}O^+$ were observed when switching from wet to dry plasma conditions, suggesting entrainment of atmospheric N_2 and CO_2 into the plasma was the dominant cause of these species as proposed by Lam and Horlick.[23] Given the low abundance of ^{70}Zn (0.60%), the presence of the $^{40}Ar^{14}N^{16}O^+$ interference effectively prevents high-precision determinations of ^{70}Zn at normal resolution ($M/\Delta M$ = 400–500).

The $^{40}Ar^{14}N^{14}N^+$ + $^{40}Ar^{12}C^{16}O^+$ interference contribution has been observed on the Axiom using off-peak baseline

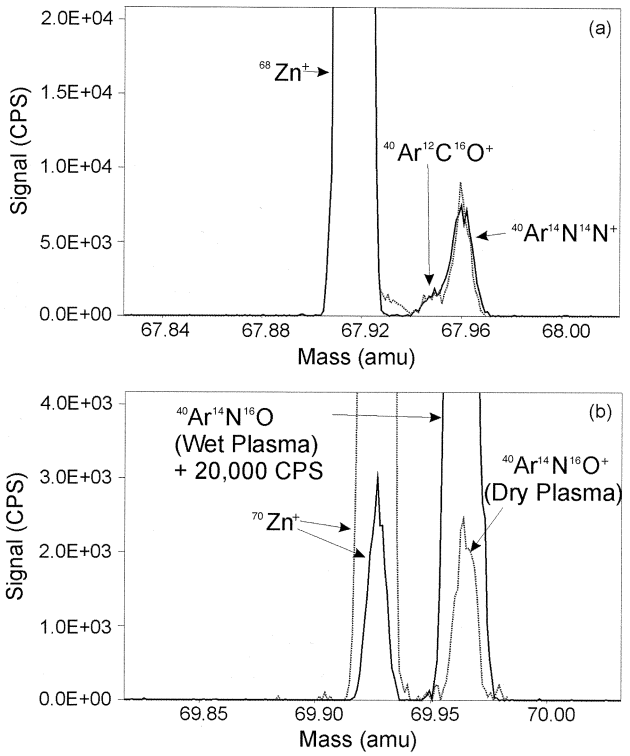

Fig. 1 Mass scans across (a) ^{68}amu and (b) ^{70}amu for a 2% (v/v) HNO_3 acid blank run on the Axiom. Measurements were made using wet (in black) and dry (in grey) plasma conditions at a spectral resolution setting of $M/\Delta M = 4500$. Spectral interferences are observed on the high mass side of the residual ^{68}Zn and ^{70}Zn peaks. These interfering species are consistent with $^{40}Ar^{12}C^{16}O^+$ and $^{40}Ar^{14}N^{14}N^+$ on ^{68}amu and $^{40}Ar^{14}N^{16}O^+$ on ^{70}amu.

corrected 0.2% HNO_3 acid blank data, whereby $^{68}Zn/^{66}Zn$ ratios were significantly greater than natural abundance Zn values. By contrast, with the IsoProbe consistency between off-peak baseline corrected $^{66}Zn/^{64}Zn$ and $^{68}Zn/^{64}Zn$ acid blank data collected under both wet and dry plasma conditions suggests $^{40}Ar^{14}N^{14}N^+$ and $^{40}Ar^{12}C^{16}O^+$ contributions at ^{68}amu are minimal. This may be tentatively explained by the dissociation of argon-based polyatomics following collisions with impurities within the hexapole collision cell,[24–26] and provides evidence that differences in MC-ICP-MS design influence background interference contributions in the Cu–Zn mass range.

Background interferences—acid matrix-related polyatomics

Polyatomic species originating from the sample introduction acid matrix are a common feature in ICP-MS analysis.[27] For HCl, H_2SO_4 and H_3PO_4, major polyatomic interferences coincide with several of the isotopes of Cu and Zn including $^{31}P^{16}O^{16}O^+$ at ^{63}amu, $^{32}S^{16}O^{16}O^+$ at ^{64}amu, and $^{35}Cl^{16}O^{16}O^+$ at ^{67}amu (see Table 1). Measurements on both instruments have shown these species persist under wet and dry plasma conditions, and as a consequence none of these acids are suitable for Cu and Zn isotope measurements. By contrast, HNO_3 produces relatively interference free spectra on both instruments, although there are some exceptions.

When running a 2% (v/v) HNO_3 blank on the Axiom under wet plasma conditions, interferences were observed on the high mass side of residual ^{64}Zn and ^{66}Zn peaks (equal to *ca.* 0.4 mV and *ca.* 0.04 mV respectively at $M/\Delta M = 400$, see Fig. 2). These decreased by an order of magnitude when reducing the concentration of the acid to 0.2% (v/v) (see Fig. 2), and were eliminated using a desolvating nebuliser (data not shown), suggesting the interferences incorporate components

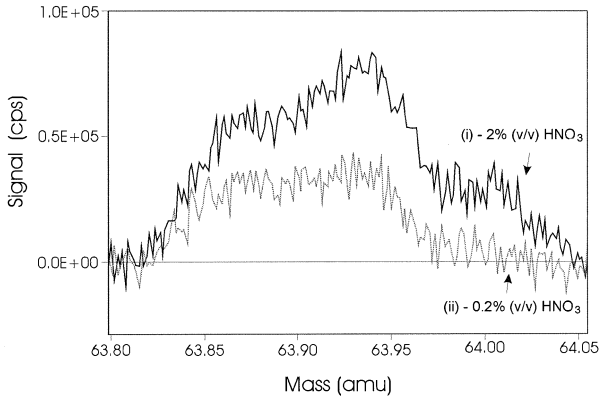

Fig. 2 Mass scan across ^{64}amu for (i) a 2% (v/v) ultra-pure HNO_3 acid blank (in black) and (ii) a 0.2% (v/v) ultra-pure HNO_3 acid blank (in grey) run on the Axiom. Measurements were made using wet plasma conditions at a spectral resolution of $M/\Delta M = 400$. With the 2% (v/v) acid blank, an interference is present on the high mass side of the residual Zn peak. This interference is reduced by an order of magnitude when the acid concentration is changed to 0.2% (v/v). This is consistent with a $^1H_2{}^{14}N^{16}O^{16}O^{16}O^+$ interference forming from constituents in the nitric acid matrix.

from the acid matrix. The relatively high masses of these species compared to residual Zn peaks are consistent with the formation of $^1H_2{}^{14}N^{16}O^{16}O^{16}O^+$ and $^1H_2{}^{14}N^{18}O^{16}O^{16}O^+$ complexes in the ICP source and/or interface region of the Axiom.

Nitric acid related interferences were not observed on the IsoProbe under wet plasma conditions (which if present would produce a marked shoulder on the up-mass side of the residual Zn peak at a mass resolution of $M/\Delta M = 500$), and such interferences have not been previously reported. Thus the formation and persistence of $^1H_2{}^{14}N^{16}O^{16}O^{16}O^+$ and $^1H_2{}^{14}N^{18}O^{16}O^{16}O^+$ appears to be a feature of the instrumental set-up used on the Axiom. For routine wet plasma isotope measurements on the Axiom in 0.2% (v/v) HNO_3, these interferences are dwarfed by the ion beams used (*e.g.* 4 V on ^{64}Zn and 2 V on ^{66}Zn), and with an on-peak zero procedure they do not influence isotope measurements of Zn.

Sample-related interferences—hydride polyatomics

Analysis of a pure 1 μg ml^{-1} Zn solution on the Axiom under wet plasma conditions revealed small but significant interferences at ^{65}amu and ^{69}amu, accounting for *ca.* 0.85 mV and *ca.* 0.35 mV, respectively. Off-peak baseline corrected data indicate these interferences are not related to peak-tailing effects, and constitute real spectral features. Furthermore, under dry plasma conditions the interferences were eliminated. This behaviour is consistent with the formation of $^{64}Zn^1H^+$ and $^{68}Zn^1H^+$ species; their removal under dry plasma conditions reflecting two possible processes: (1) a relative reduction in $^1H^+$ atoms entering the plasma due to the desolvation process, and/or (2) increased instability of ZnH^+ species in the hotter dry plasma resulting in their decay, both of which have been invoked to explain the reduction in oxide interferences when changing from wet to dry plasma conditions.[28,29]

The presence of $^{64}Zn^1H^+$ has important implications for simultaneous Cu and Zn measurements as changes in the [Cu]/[Zn] ratio will alter the relative proportion of $^{64}Zn^1H^+$ to $^{65}Cu^+$, thus shifting the measured $^{65}Cu/^{63}Cu$ ratio. To quantify this effect, the $^{65}Cu/^{63}Cu$ ratio of the NIST Cu standard was measured at various concentrations (0.2, 0.02, 0.01, 0.002 μg ml^{-1}) while maintaining a constant Zn concentration (0.5 μg ml^{-1}). The results are presented in Fig. 3. These data have been mass discrimination corrected using the empirical

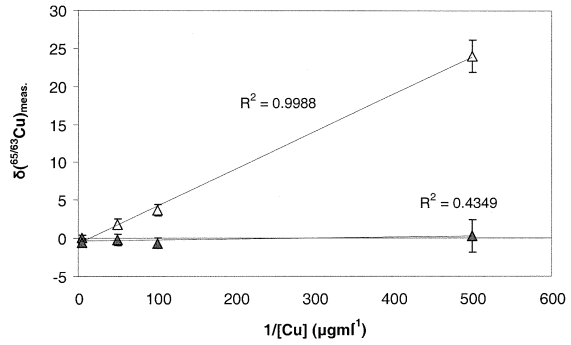

Fig. 3 Variation in $\delta^{65/63}$Cu with [Cu] for a series of NIST Cu solutions spiked with 1 μg ml^{-1} IMP Zn. These measurements were made using wet plasma conditions on the Axiom and all data have been baseline corrected using an on-peak zero procedure. All $\delta^{65/63}$Cu data are relative to the measured composition of a 0.4 μg ml^{-1} NIST Cu solution. The hollow symbols represent the raw data and the solid symbols represent the ZnH^+ corrected data. Data have been regressed using a least mean square regression; 2σ error bars are included.

external normalisation approach with Zn as an internal standard.[12] The raw data, presented using δ-notation where $\delta^{65/63}Cu = [(^{65}Cu/^{63}Cu)_{samp}/(^{65}Cu/^{63}Cu)_{std} - 1] \times 1000$ (‰) for each solution (samp.) relative to the composition of the starting 0.2 μg ml^{-1} Cu solution (std.), define a mixing line between the $^{64}Zn^1H^+$ interference on ^{65}Cu and the isotopic composition of the Cu solution analysed. Thus even relatively small changes in the [Cu]/[Zn] ratio between samples and standards of a few percent can induce significant isotopic shifts in the measured $^{65}Cu/^{63}Cu$ ratio.

Continued monitoring of the $^{64}ZnH^+/^{64}Zn^+$ ratio over a two-week period has shown the ZnH^+ generation rate is relatively constant for individual measurement sessions (with a typical value of $^{64}ZnH^+/^{64}Zn^+ = 0.000096 \pm 0.000004$ (2σ)), but can change significantly between sessions by up to a factor of two or more. The shifts between measurement sessions likely reflect differences in the plasma gas flow settings that are known to influence the generation rates of other interferences, *e.g.* doubly charged ions,[27] argide and oxide interferences.[30] Given this within session stability, it is possible to measure relative isotopic differences between unknown samples and standards using a concentration matching protocol. However, this can be time-consuming for unknown samples. A correction procedure for ZnH^+ has thus been developed whereby a 1 μg ml^{-1} Zn solution is analysed directly before each sample/standard analysis from which the associated $^{64}ZnH^+/^{64}Zn^+$ ratio is calculated. These values are then used to quantify and correct how much ZnH^+ was generated by each down mass Zn peak during the subsequent sample/standard analysis. The ZnH^+ correction has been applied to the data in Fig. 3. Here the correction effectively brings all of the measured values back to the starting composition, illustrating the success of the approach. Alternatively, measurements can be made using dry plasma conditions where ZnH^+ does not form in significant quantities.

No significant $^{63}Cu^1H^+$ or $^{65}Cu^1H^+$ interferences were observed on the Axiom under either wet or dry plasma conditions. It is unclear why Cu and Zn should behave differently with respect to hydride formation, although this may reflect differences in the dissociation energies of CuH^+ and ZnH^+ species within the ICP-source, as has been suggested for elemental trends in metal argide formation in ICP-MS.[31,32] Measurements on the IsoProbe have also failed to identify any significant ZnH^+ or CuH^+ interferences above background noise. Previous studies using a VG Elemental Plasma-54 for simultaneous Cu and Zn measurements using wet plasma conditions also reported no significant hydride generation,[6] suggesting the observed ZnH^+ production is specific to the instrumental set-up used on the Axiom.

Sample-related interferences—matrix components

The results of a series of experiments to evaluate the influence of polyatomic spectral interferences incorporating Na, Mg, Al, Ti, V, Cr, Ba and Ce on $^{65}Cu/^{63}Cu$, $^{66}Zn/^{64}Zn$, $^{67}Zn/^{64}Zn$ and $^{68}Zn/^{64}Zn$ ratio measurements are presented in Fig. 4. These data represent the per mil (‰) deviation associated with the addition of the specified element of each measured ratio away from the isotopic composition of the unspiked Cu + Zn standard solution, where Cu, Zn and the contaminant element are in equal proportions. For example, from Fig. 4(a), the addition of 1 μg ml^{-1} Na to a solution of 1 μg ml^{-1} Cu and 1 μg ml^{-1} Zn shifts the $^{65}Cu/^{63}Cu$ ratio by −0.5‰. This is consistent with the formation of a Na polyatomic species ($^{23}Na^{40}Ar^+$) on ^{63}amu. Data on S, P, Si and Te are not presented, as the spectral interferences associated with these elements were too small (<0.2‰ of the corresponding isotope ratio) to be identified with confidence.

Matrix-related interference contributions on the Axiom and IsoProbe show increasing significance from argides ($NaAr^+$, $MgAr^+$, $AlAr^+$) to oxide/hydroxide (TiO^+, $TiOH^+$, VO^+, VOH^+, CrO^+, $CrOH^+$) to double-charged species (Ba^{2+}, Ce^{2+}) (see Fig. 4). These data predict trace element constituents within the analyte solution will have a disproportionately large influence on high-precision Cu and Zn isotope measurements relative to major element components. However, these trends are not universal. For example, no $^{126}Te^{2+}$, $^{128}Te^{2+}$ and $^{130}Te^{2+}$ interferences were observed above instrumental backgrounds on either the IsoProbe or the Axiom under wet or dry plasma conditions for a 1 μg ml^{-1} Te solution (data not shown), which contrasts with Ba and Ce that readily form double-charged species. This decoupled behaviour is consistent with the relatively high second order ionisation potential of Te (1790 kJ mol^{-1})[33] compared to Ba (965.2 kJ mol^{-1})[33] and Ce (1050 kJ mol^{-1}),[33] which prevents significant Te^{2+} formation in the ICP-source.

The relative interference contribution also depends upon the sample introduction system used, as depicted by the solid (wet plasma) and patterned (dry plasma) bars in Fig. 4. Argide and doubly-charged interferences increase from wet to dry plasma conditions by a factor of 1.5–5 on both instruments. The increase in the former may reflect an enhancement in secondary discharge in the interface region which is believed to control argide formation,[30] while the observed increase in double-charged ions is consistent with an increase in the temperature and subsequently the ionisation efficiency of the dry plasma. Conversely, oxide interferences are reduced by an order of magnitude from wet to dry plasma conditions. This may indicate a reduction in the density of oxygen atoms in the ICP-source due to the desolvation process,[29] and/or an increase in the temperature of the ICP-source which favours dissociation of the oxide ions in the plasma.[28]

Despite the different experimental approaches employed to evaluate the interference contributions for major and trace elements on the Axiom and IsoProbe (see Experimental section), the similarity between the interference contributions for the two instruments is remarkable. Both the Axiom and IsoProbe show the same pattern for wet and dry plasma conditions, suggesting the dominant processes controlling the formation and persistence of argide, oxide and double-charge interferences are essentially the same for the two instruments. Furthermore, the formation and/or persistence of matrix-related polyatomic species do not appear to be significantly affected by either the inclusion of an argon-bled hexapole collision cell in the IsoProbe, or differences in interface design between the two instruments. This result is surprising given the clearly different behaviours of $^{40}Ar^{14}N^{14}N^+$, $^{40}Ar^{12}C^{16}O^+$ and Zn^1H^+-related species on the two instruments. We cannot as yet explain this discrepancy, which merits further investigation.

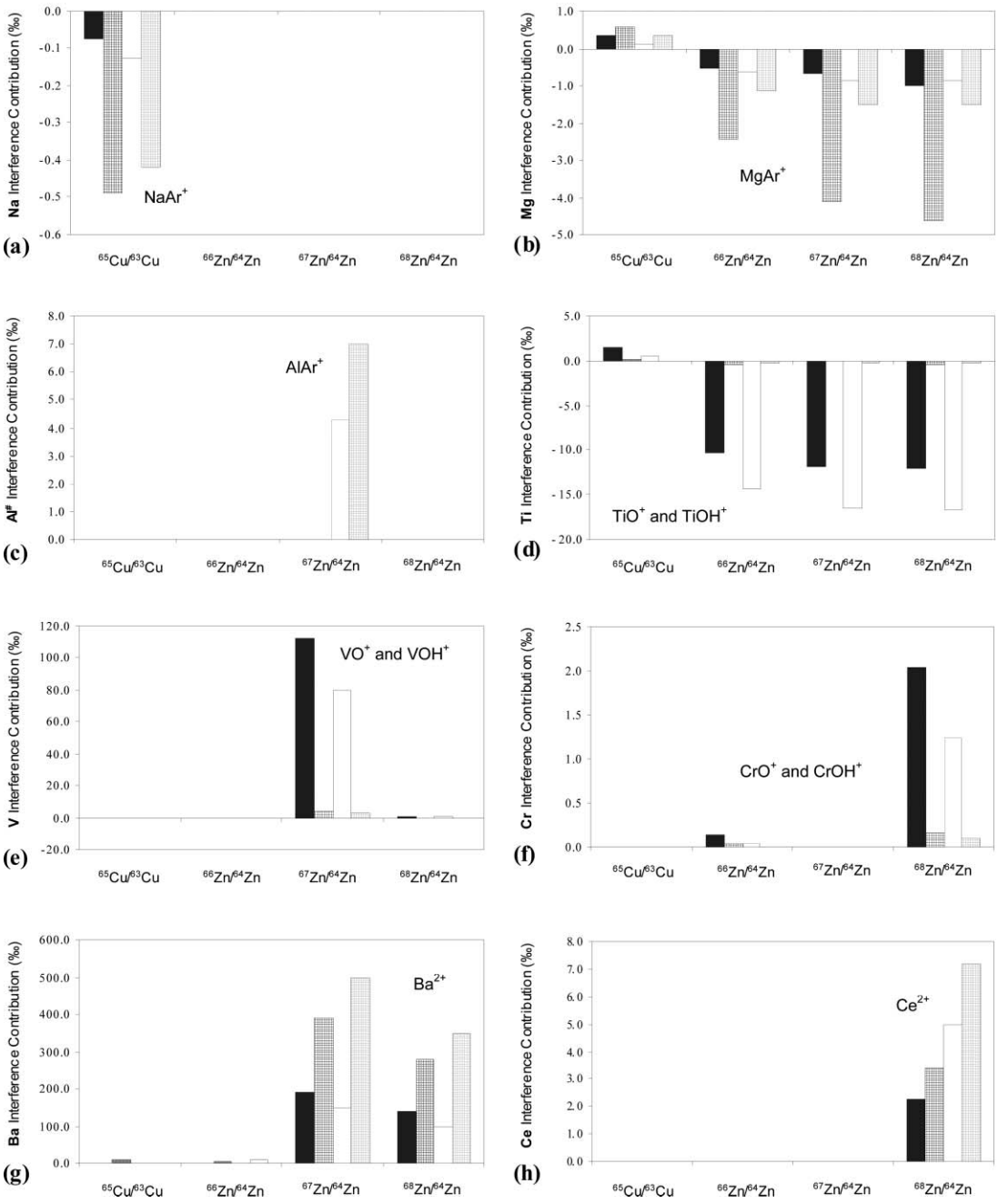

Fig. 4 Per mil variations induced in $^{65}Cu/^{63}Cu$, $^{66}Zn/^{64}Zn$, $^{67}Zn/^{64}Zn$ and $^{68}Zn/^{64}Zn$ ratios by the addition of equal concentrations of (a) Na, (b) Mg, (c) Al, (d) Ti, (e) V, (f) Cr, (g) Ba and (h) Ce relative to a solution of 1 μg ml^{-1} IMP Cu + 1 μg ml^{-1} IMP Zn. These shifts are indicative of the formation of polyatomic species incorporating the specified element. Data collected on the IsoProbe are given in dark grey and data collected on the Axiom are given in pale grey. Wet plasma measurements are represented by the single colouration, and dry plasma measurements are represented by the chequered colouration. For Al, data from the IsoProbe is not reported due to suspected non-spectral effects.

Correcting for instrumental and acid blank related interferences

Instrumental and acid blank related interferences are prevalent in the Cu–Zn mass range on both the Axiom and IsoProbe. If these interferences maintain a constant ratio with analyte sensitivity throughout a measurement session, a concentration matching protocol should theoretically be insensitive to background contributions, enabling high-precision Cu and Zn isotopic measurements to be undertaken. However, concentration matching unknown samples is not always convenient or possible.

An on-peak baseline correction offers the ability to correct instrumental and acid blank interference contributions directly, circumventing the need for a concentration matching protocol. To assess this approach, $^{66}Zn/^{64}Zn$ data were collected on the IMP Zn standard, measured over a range of concentrations (from 0.5 to 0.004 μg ml^{-1} Zn) on both the Axiom and IsoProbe, under wet and dry plasma conditions. These data were baseline corrected using the on-peak zero procedure and an off-peak baseline correction, and the data were mass discrimination corrected using the empirical external normalisation correction with Cu the mass discrimination monitor.[12]

The results are given in Fig. 5 using δ-notation relative to the average measured composition of a 1 μg ml^{-1} IMP Zn solution analysed during the same analytical session. With the IsoProbe, off-peak baseline corrected Zn isotope data (as depicted by solid triangles in Fig. 5(a)) show a significant correlation with 1/[Zn] ($R^2 = 0.997$, $n = 5$). This is interpreted as a mixing line between the IMP Zn standard and an instrumental interference contribution on ^{64}amu. In contrast, the on-peak baseline corrected data (as depicted by open triangles in Fig. 5(a)) show

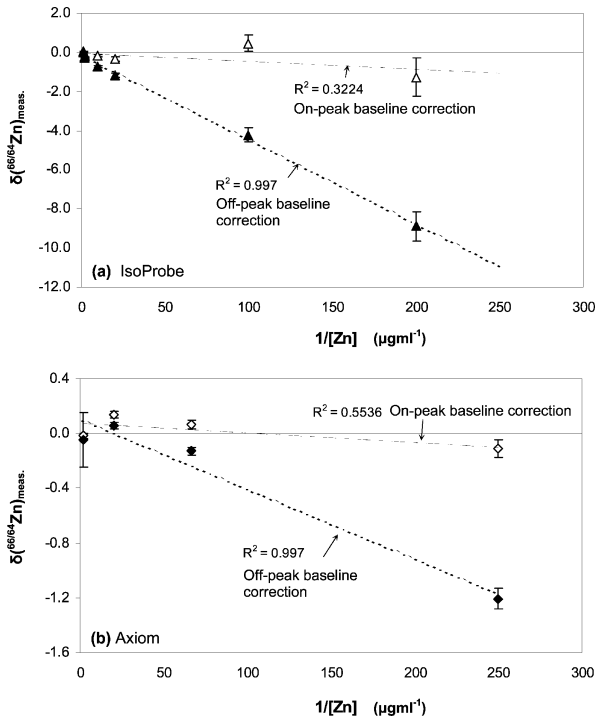

Fig. 5 Variation in $\delta^{66/64}$Zn with [Zn] for a series of IMP Zn solutions spiked with 0.4 μg ml^{-1} IMP Cu. All data were collected using wet plasma conditions on (a) the IsoProbe (triangles) and (b) the Axiom (diamonds). All $\delta^{66/64}$Zn/^{64}Zn values are relative to the average isotopic composition of 1 μg ml^{-1} IMP Zn + 0.4 μg ml^{-1} IMP Cu solution run during the same analytical session. Two baseline corrections were used: (1) an off-peak baseline correction (solid symbols) and (2) an on-peak 0.2% HNO_3 acid blank subtraction (open symbols). Least mean square regressions have been fitted to the off-peak baseline corrected data. Error bars represent ±2 standard errors (SE) for $n = 100$ sample integrations.

no statistical correlation with 1/[Zn] ($R^2 = 0.322$, $n = 5$), showing the instrumental interference contribution at ^{64}amu is effectively eliminated using the on-peak correction. Similar results were obtained with the Axiom (Fig. 5(b)), although the deviations here are significantly less pronounced due to the reduced instrumental Ni contribution. These data illustrate the application of an on-peak baseline subtraction procedure where instrumental and acid blank contributions are present.

The errors associated with these measurements are significantly greater on the IsoProbe (up to ±1‰ (2SE)) when compared to the Axiom (up to ±0.075‰ (2SE)) (Fig. 5), and these errors are not significantly reduced when applying a simultaneous ^{64}Ni-correction (data not shown). This deterioration in measurement precision is consistent with temporal fluctuations in the as yet unidentified interference contribution to ^{64}amu on the IsoProbe. Thus, although the on-peak baseline correction can adequately account for the bulk effects of the instrumental and acid blank background contribution, it does not correct for short-term variations in the background contribution.

Summary

Significant ^{64}Ni backgrounds occur on the Axiom and IsoProbe. These increase when switching from wet to dry plasma conditions and are proposed to reflect streaming of Ni off components used in the interface.

An as yet unidentified interference contribution occurs at ^{64}amu on the IsoProbe. This is insensitive to the sample introduction system used and does not relate to $^{40}Ar^{24}Mg^+$, $^{36}Ar^{28}Si^+$, $^{48}Ca^{16}O^+$, $^{48}Ti^{16}O^+$, $^{32}S^{16}O^{16}O^+$, $^{32}S^{32}S^+$, $^{128}Xe^{2+}$ or $^{40}Ar^{12}C^{12}C^+$ species. We tentatively link this contribution to O_4^+ species originating from water within the hexapole collision cell.

$^{40}Ar^{14}N^{14}N^+$ and $^{40}Ar^{12}C^{16}O^+$ polyatomics on ^{68}amu plus HNO_3-related $^1H_2{}^{14}N^{16}O^{16}O^{16}O^+$ and $^1H_2{}^{14}N^{18}O^{16}O^{16}O^+$ species on ^{64}amu and ^{66}amu occur on the Axiom. These species were not observed on the IsoProbe, possibly reflecting the dissociation of such species through ion-molecule reactions within the hexapole collision cell.

Zinc hydride polyatomics have been identified on the Axiom under wet plasma conditions. These species have been successfully corrected by monitoring the $^{64}ZnH^+/^{64}Zn^+$ ratio and applying an off-line peak subtraction, and are eliminated using a desolvated plasma. By contrast, ZnH^+ species were not observed on the IsoProbe, and CuH^+ species have not been recognised on either instrument.

Matrix-induced interference contributions on the Axiom and IsoProbe show increasing significance from argides ($NaAr^+$, $MgAr^+$, $AlAr^+$) to oxide/hydroxide (TiO^+, $TiOH^+$, VO^+, VOH^+, CrO^+, $CrOH^+$) to double-charged species (Ba^{2+}, Ce^{2+}). Switching from solution nebulisation to a desolvated plasma enhances argide and double-charged species, and concurrently depresses oxides and hydroxides, reflecting changing conditions within the ICP-source.

An on-peak baseline correction has been successfully used to correct for instrumental background contributions on both the Axiom and IsoProbe. However, this correction does not account for sample matrix-related components, requiring problematic components such as Na, Mg, Al, Ti, Cr, V, Ba and Ce to be removed prior to Cu and Zn isotope measurements.

Acknowledgements

We wish to thank the Natural Environmental Research Council (NERC) for ongoing support of the laboratory facilities used during the study and for funding the CASE PhD scholarship under which this work was undertaken. We are very grateful to C. P. Ingle, G. Nowell, R. McGill and V. Pashley who all contributed to the analyses on the Axiom. A. Dolgopolova, M. Gounelle, T. Jeffries, V. Din, G. Jones, C. Smith and T. Williams are thanked for their help in running and maintaining the IsoProbe as part of the NHM/IC JAF. Prof. I. Thornton and Prof. M. M. E. Farrago are thanked for their interest in the project. Finally we wish to acknowledge Professor A. Fleet, M. Warner and the Leverhulme Trust for helping finance this work.

References

1 A. J. Walder and P. A. Freedman, *J. Anal. At. Spectrom.*, 1992, **7**, 571.
2 A. N. Halliday, D. C. Lee, J. N. Christensen, A. J. Walder, P. A. Freedman, C. E. Jones, C. M. Hall, W. Yi and D. Teagle, *Int. J. Mass Spectrom. Ion Processes*, 1995, **146**, 21.
3 M. Rehkämper, M. Schonbachler and C. H. Stirling, *Geostand. Newsl.*, 2001, **25**, 23.
4 A. N. Halliday, D. C. Lee, J. N. Christensen, M. Rehkämper, W. Yi, X. Z. Luo, C. M. Hall, C. J. Ballentine, T. Pettke and C. Stirling, *Geochim. Cosmochim. Acta*, 1998, **62**, 919.
5 N. H. Gale, A. P. Woodhead, Z. A. Stos-Gale, A. Walder and I. Bowen, *Int. J. Mass Spectrom.*, 1999, **184**, 1.
6 C. N. Maréchal, P. Télouk and F. Albarède, *Chem. Geol.*, 1999, **156**, 251.
7 C. N. Maréchal, E. Nicolas, C. Douchet and F. Albarède, *Geochem. Chem. Geosyst.*, 2000, **1**, GC000029.
8 S. Pichat, C. Douchet and F. Albarède, *Earth Planet. Sci. Lett.*, 2003, **210**, 167.
9 X. K. Zhu, R. K. O'Nions, Y. Guo, N. S. Belshaw and D. Rickard, *Chem. Geol.*, 2000, **163**, 139.
10 D. Vance and M. Thirlwall, *Chem. Geol.*, 2002, **185**, 227.
11 M. Thirlwall, *J. Anal. At. Spectrom.*, 2001, **16**, 1121.
12 T. F. D. Mason, D. J. Weiss, M. Horstwood, R. R. Parrish, S. S. Russell, E. Mullane and B. J. Coles, *J. Anal. At. Spectrom.*; DOI: 10.1039/b306953b.
13 A. T. Townsend, *J. Anal. At. Spectrom.*, 2000, **15**, 307.

14 A. T. Townsend, K. A. Miller, S. McLean and S. Aldous, *J. Anal. At. Spectrom.*, 1998, **13**, 1213.
15 F. Vanhaecke, L. Moens and R. Dams, *J. Anal. At. Spectrom.*, 1998, **13**, 1189.
16 I. Rodushkin and T. Ruth, *J. Anal. At. Spectrom.*, 1997, **12**, 1181.
17 C. Barbante, T. Bellomi, G. Mezzadri, P. Cescon, G. Scarponi, C. Morel, S. Jay, K. VanDeVelde, C. Ferrari and C. F. Boutron, *J. Anal. At. Spectrom.*, 1997, **12**, 925.
18 J. Riondato, F. Vanhaecke, L. Moens and R. Dams, *J. Anal. At. Spectrom.*, 2000, **15**, 341.
19 B. Hattendorf and D. Günther, *J. Anal. At. Spectrom.*, 2000, **15**, 1125.
20 Y. Shao and G. Horlick, *Appl. Spectrosc.*, 1991, **45**, 143.
21 K. J. R. Rosman and P. D. P. Taylor, *J. Anal. At. Spectrom.*, 1998, **13**, 45N.
22 P. D. P. Taylor, P. Debievre, A. J. Walder and A. Entwistle, *J. Anal. At. Spectrom.*, 1995, **10**, 395.
23 J. Lam and G. Horlick, *Spectrochim. Acta, Part B*, 1990, **45**, 1327.
24 S. D. Tanner, V. I. Baranov and D. R. Bandura, *Spectrochim. Acta, Part B*, 2002, **57**, 1361.
25 C. J. Barinaga and D. W. Koppenall, *Rapid Commun. Mass Spectrom.*, 1994, **8**, 71.
26 P. D. P. Turner, T. Merren, J. Speakman and C. Haines, in *Plasma Source Mass Spectrometry: Developments and Applications*, ed. S. D. Tanner, Royal Society of Chemistry Special Publication, Cambridge, 1997.
27 A. L. Gray, *Spectrochim. Acta, Part B*, 1986, **41**, 151.
28 P. S. Clemons, M. G. Minnich and R. S. Houk, *Anal. Chem.*, 1995, **67**, 1929.
29 L. C. Alves, D. R. Weiderin and R. S. Houk, *Anal. Chem.*, 1992, **64**, 1164.
30 N. S. Nonose, N. Matsuda, N. Fudagawa and M. Kubota, *Spectrochim. Acta, Part B*, 1994, **49**, 955.
31 C. W. Bauschlicher, H. Partridge and S. R. Langhoff, *Chem. Phys. Lett.*, 1990, **165**, 272.
32 J. S. Becker, G. Seifert, A. I. Saprykin and H. J. Dietze, *J. Anal. At. Spectrom.*, 1996, **11**, 643.
33 A. M. James and M. P. Lord, *Macmillan's Chemical and Physical Data*, Nature Publishing Group, London, 1992.